Available online at www.sciencedirect.com

ScienceDirect

Advances in Space Research 71 (2023) 160–175

ADVANCES IN SPACE RESEARCH
(a COSPAR publication)

www.elsevier.com/locate/asr

Investigation of gravity wave characteristics in the equatorial ionosphere during the passage of the 15 January 2010 solar eclipse over Tirunelveli

Rajesh Kumar Barad, S. Sripathi *

Indian Institute of Geomagnetism, Plot-5, Sector-18, New Panvel, Navi Mumbai 410218, India

Received 25 April 2022; received in revised form 18 August 2022; accepted 22 August 2022
Available online 27 August 2022

Abstract

Solar eclipses are known to produce gravity wave disturbances in the atmosphere–ionosphere system in addition to density reduction due to temporary changes in solar radiation. The magnetic equator is ideally located to investigate these waves and their coupling to the equatorial ionosphere due to its unique geometry. Accordingly, the response of the equatorial ionosphere to a rare Annular Solar Eclipse (ASE) observed on 15 January 2010 is investigated using high-resolution observations from Canadian Advanced Digital Ionosonde (CADI) located at Tirunelveli which is a magnetic equator and on the eclipse totality path in India. In addition, simultaneous observations of GPS TEC from Tirunelveli, electron density profiles from Constellation Observing System for Meteorology Ionosphere and Climate (COSMIC), and Equatorial Electrojet (EEJ) strength were analysed. The real height analysis has been performed on the ionosonde data using POLynomial ANalysis (POLAN). The isoheight/isofrequency analysis has been performed using real height on eclipse and control days. The results indicate a reduction of ~33% in the lower ionosphere whereas no change has been noticed close to the F layer peak on the eclipse day. The isoheight analysis further indicates the presence of gravity waves with dominant periods in the range of 5–30 min. Further analyses have been performed on the altitude variation of dominant waves and their amplitudes/phases using ionosonde to identify whether they are generated in situ or propagated from below. The altitude variation of group and phase velocities showed opposite propagation indicating that they were propagated from the below. In addition, the simultaneous presence of gravity waves in the fmin, TEC, and EEJ strength on eclipse day supports our finding that these waves were propagated from the lower atmosphere.

Keywords: Solar eclipses; Gravity waves; Fmin; Equatorial ionosphere; Ionosonde observations; GPS TEC observations

1. Introduction

The solar eclipse occurs in a peculiar geometry, where the Sun, Earth, and Moon align in a straight line that happens normally during a new moon resulting in the passage of the Moons shadow at supersonic speed on the Earth (Chimonas and Hines, 1970). The solar eclipse can be classified as total, annular or partial depending on the distance between the Earth and the Moon. The solar eclipse provides an opportunity to test various theories and hypotheses and their induced disturbances in the atmosphere/ionosphere. Accordingly, the impact of the solar eclipses on the earth's atmosphere and ionosphere has been investigated extensively using a variety of measuring techniques such as radiosondes, ionosondes, coherent and incoherent scattering radars, geomagnetic field variations, Faraday rotation techniques, and GPS TEC observations (Evans, 1965a; Evans, 1965b; Rishbeth, 1968; Bamford, 2001). As the moon's shadow passes through the earth, it causes temporary cooling in the atmosphere and as it moves at the supersonic speed (M > 2), it

* Corresponding author.
E-mail address: ssripathi.iig@gmail.com (S. Sripathi).

https://doi.org/10.1016/j.asr.2022.08.059
0273-1177/

produces bow shock waves similar to the waves generated by the sailing boat (Chimonas and Hines, 1970; Zhang et al., 2017). Past studies have indicated that solar eclipses can impact the ionosphere mainly through the sudden reduction of photoionization and occurrence of gravity waves in the ionosphere (Van Zandt et al., 1960; Chimonas and Hines, 1970). Chimonas and Hines (1971) have studied the passage of eclipses using both observations and theory and predicted that fast moving moon's shadow can produce acoustic waves and gravity waves at the surface and stratospheric altitudes due to sudden local cooling surrounded by heating of the stratosphere. While few experimental results confirm that such waves do propagate from the stratospheric altitude to the ionosphere during eclipse passages (Davis and Da Rosa, 1970; Fritts and Luo, 1993), few others suggest that these could be generated in situ in the ionosphere itself (Müller-Wodarg et al., 1998; Altadill et al., 2001b; Manju et al., 2012). Recent studies have suggested that gravity waves can be excited in both stratosphere and ionosphere simultaneously during solar eclipses (Šauli et al., 2007). Sometimes other natural phenomena such as geomagnetic storms and tidal variability mask their signatures and hence the difficulty in identifying their sources. Accordingly, the issue of the origin of these waves such as whether they are excited in the stratosphere/troposphere or in situ generated in the ionosphere is still not addressed and hence there is a scope for further studies. As the gravity waves propagate from troposphere/stratosphere to ionospheric altitudes, the wave amplitude also increases significantly due to reduced density resulting in the production of travelling ionospheric disturbances (TIDs) in those altitudes through the interaction of propagating neutral waves with ionization density. These disturbances are having periods in the range of 20 to 40 min. During a solar eclipse, the moon's shadow is observed as temporary 'darkness' or 'night' on the earth. This darkness on the earth is extended for longer durations if eclipse magnitude maximizes. Due to this temporary darkness, the ionosphere experiences sudden cooling and the density drops significantly. Solar eclipse produces maximum effects around local noon than evening and morning when solar radiation is found to be significant (Le et al., 2008). Studies suggest that the eclipse effect is stronger in the E and F1 layers than in the F2 layer due to faster recombination in these regions (Bamford, 2001). While the lower part of the ionosphere is affected by the production and loss processes, the upper part of the ionosphere is additionally affected by the transport process through downward diffusion.

The impact of solar eclipses has been studied across many locations, while the passage of eclipses over magnetic equatorial regions is of special significance due to its unique geometry where the earth's magnetic field lines are not only horizontal but also perpendicular to the primary zonal electric field that is produced by the lower atmospheric wave dynamics (Sridharan et al., 2002). The equatorial ionosphere is, hence, ideally placed to observe a variety of physical processes that couple the lower atmospheric processes to the upper atmosphere through winds, waves, and tides, and modifies the primary zonal electric field. The primary electric field again produces the equatorial fountain effect at crest and trough regions under geomagnetically quiet conditions. However, it is believed that the solar eclipse potentially modifies the said quiet-time behaviour temporarily due to sudden modifications in the electric fields, ionization density, and composition due to sudden modifications in the ionization and recombination rates. The daytime conditions could be suddenly reversed to 'nighttime' conditions, and it is expected to drive Pre-Reversal Enhancement (PRE) in the zonal electric field that can lead to the development of plasma irregularities and additional layers. It is expected that these plasma density irregularities and additional layers are driven by eclipse-induced density gradients under favourable recombination, winds, and wind shear conditions (Patra and Choudhary, 2009). So, it is always exciting to examine the response of the equatorial ionosphere to such rare events as they provide a unique opportunity. The Great American Eclipse of 21 August 2017 has attracted huge attention in the recent past as Americans have witnessed a total solar eclipse for the first time after nearly 100 years. Co-ordinated campaigns were conducted using several scientific instruments across the eclipse path in addition to the modelling studies that produced many interesting aspects such as the passage of bow waves, TIDs, reduction of E and F region density (Zhang et al., 2017).

Motivated by the studies from the great American eclipse and other such eclipses in the recent past, we analysed the behaviour of the equatorial ionosphere for gravity waves on 15 January 2010 over Tirunelveli where the maximum eclipse effects have been seen due to its alignment with the totality path. This eclipse is maximized for nearly 10 min in the Maldives at annularity which is close to southern India. In India, this eclipse passes through the southern tip. The eclipse started at 05:41 UT (11:11 IST; IST = UT + 5.5) at Tirunelveli and ended at 09:30 UT (15:08 IST) maximum observed at 13:20 IST with 92% magnitude. The eclipse lasted for nearly 3 h, 57 min. Several coordinated campaigns using radars, magnetometers, GPS receivers, rockets, and ionosondes have been carried out over the Indian sector to investigate the neutral and ionized density variations for this event (Taori et al., 2010; St.-Maurice et al., 2011; Dutta et al., 2011; Patra et al., 2011; Choudhary et al., 2011; Manju et al., 2012; Nayak et al., 2012; Vyas and Sunda, 2012; Manju et al., 2014; Panda et al., 2015). Several interesting results have been brought out due to this solar eclipse event, still, no clear evidence exists if gravity waves are excited in situ or propagated from the stratosphere due to which better explanation is required. As Moon is closer to the Earth during northern winter due to the rotation of the earth, the eclipse that occurred during winter on 15 January 2010 is also believed to be influenced by the strong lunar tidal effect. Though this solar eclipse event has been explored well in the past using ground based GPS TEC, geomagnetic field variations, and ionosondes, most of these results reported mainly the reduction of density and role of the wind system that produced counter electrojet. St.-Maurice et al. (2011) suggested that an eclipse-induced westward electric field can induce counter electrojet (CEJ) during the eclipse. Jakowski et al. (2008) have studied the effects of the 3 October 2005 solar eclipse using vertical incidence sounding (VS), High Frequency Doppler, and TEC measurements. The TEC observations showed a decrease of approximately 30% during the eclipse event. The VS and HF Doppler observations showed the generation of atmospheric gravity waves in the thermosphere at around 180 km. Manju et al. (2012) has presented an investigation into gravity waves using combined ionosonde and rocket observations over Trivandrum which is 100 km far from Tirunelveli. In this paper, we examine this problem using ionosonde to investigate the origin of density perturbations as it is seen that one of the key aspects in eclipse studies is to identify whether these gravity waves are excited from the troposphere/stratosphere or in situ generated. We use additional supportive observations such as GPS TEC, Constellation Observing System for Meteorology Ionosphere and Climate (COSMIC) density profiles, and Equatorial Electrojet (EEJ) strength in this study to provide comprehensive results and insights into the analysis of this eclipse. Using these observations, the propagation of gravity waves in the ionosphere over Tirunelveli that are excited during eclipse has been systematically investigated.

2. Description of data and methodology

The results presented in this paper are based on the data collected from CADI (Canadian Advanced Digital Ionosonde) located at Tirunelveli, an equatorial station in India along with EEJ strength data and GPS TEC observations. The CADI was operated continuously in a campaign mode at high resolution (2 min) on 14, 15, and 16 January 2010 to study the ionospheric variability due to the passage of eclipse and its gravity wave signatures. This system can run in both ionogram and Doppler modes. However, to study the gravity wave activity, the campaign was run only under ionogram mode. More details about the campaign are given in Nayak et al. (2012). It may be mentioned that year 2010 falls under moderate solar flux year and no geomagnetic storm activity is seen during this eclipse period that could mask the ionospheric response to the solar eclipse. We utilized a special type of analysis to study the impact of the eclipse on the equatorial ionosphere. We fit each ionogram manually to get density profiles of the local ionosphere with respect to real height. The density profiles are obtained using POLAN (POLynomial ANalysis) software. Further, these density profiles are subjected to isoheight and isofrequency analysis. To obtain the isoheight and isofrequency data, each density profile is binned at every 5 km from 190 to 260 km and every 0.5 MHz frequency from 4 to 6 MHz frequency respectively. This type of analysis has been utilized to study the gravity wave characteristics during solar eclipses (Altadill et al., 2001b; Koucká Knížová and Mošna, 2011; Liu et al., 1998). We also reduced the ionogram data to obtain h'F, foF1, foF2, h'E, foEs, fmin, and h'fmin during this event. In addition to ionosonde observations, data from SCIntillation Network Decision Aid (SCINDA) GPS receiver located at Tirunelveli were used for further supporting observations. The GPS TEC data for the eclipse has been widely used in the recent past to identify the acoustic gravity waves, gravity waves, and bow waves. The GPS data has been processed to obtain the TEC as per the usual procedures. TEC can be calculated by using the dispersive nature of the ionosphere for radio waves. Two radio signals of frequency L1 (1575.42 MHz) and L2 (1227.60 MHz) are transmitted from the GPS satellite. After passing through the dispersive ionosphere the code signal and carriers experience group delay and phase advance respectively. The group delay and phase advance are proportional to the total number of electrons along the line of sight of the satellite and receiver. The obtained total electron content is called as the slant total electron content (sTEC). The sTEC is converted to vertical total electron content (vTEC) using appropriate mapping function. The vTEC data having a time resolution of 1 min is used to obtain the eclipse related changes in the ionosphere. For our convenience, we assume TEC as vTEC from now onwards. EEJ strength data over the Indian sector, obtained by subtracting the H-component data from Tirunelveli and Alibag stations, is also utilized after subtracting their mid-night values to have a zero bias due to artefacts. Note that the time resolution of EEJ is 1 min. Savitzky-Golay (S-G) filtering technique is performed on EEJ, TEC, and Ionosonde data. Please note that we have applied S-G filter of order 5 and frame length 49 to all the data sets presented here so that they can be easily compared. For the S-G filtering, the order must be a positive integer but it should be less than the frame length, which is again a positive odd integer. The S-G filters are low pass filters typically used in smoothing the data based on local least-squares polynomial approximation. Here, the S-G filtering technique has been applied to extract small-scale fluctuations in the data during the time of the eclipse event to study the eclipse-induced gravity waves. This technique has been applied in various types of signal extraction techniques in many geophysical applications. The S-G filtered ionosonde data, EEJ data, and TEC data are subjected to Fast Fourier Transform (FFT) and Morlet wavelet analysis. In addition, we also utilized the COSMIC electron density profiles to study the altitude variation of electron density and its short period variations over the Indian region on the eclipse day and control days Rocken et al. (2000).

Fig. 1 shows the path of the 15 January 2010 solar eclipse over the Indian region. In the figure, the red triangle is the Tirunelveli station from which we have collected the ionosonde, GPS TEC, and geomagnetic data. The blue tri-

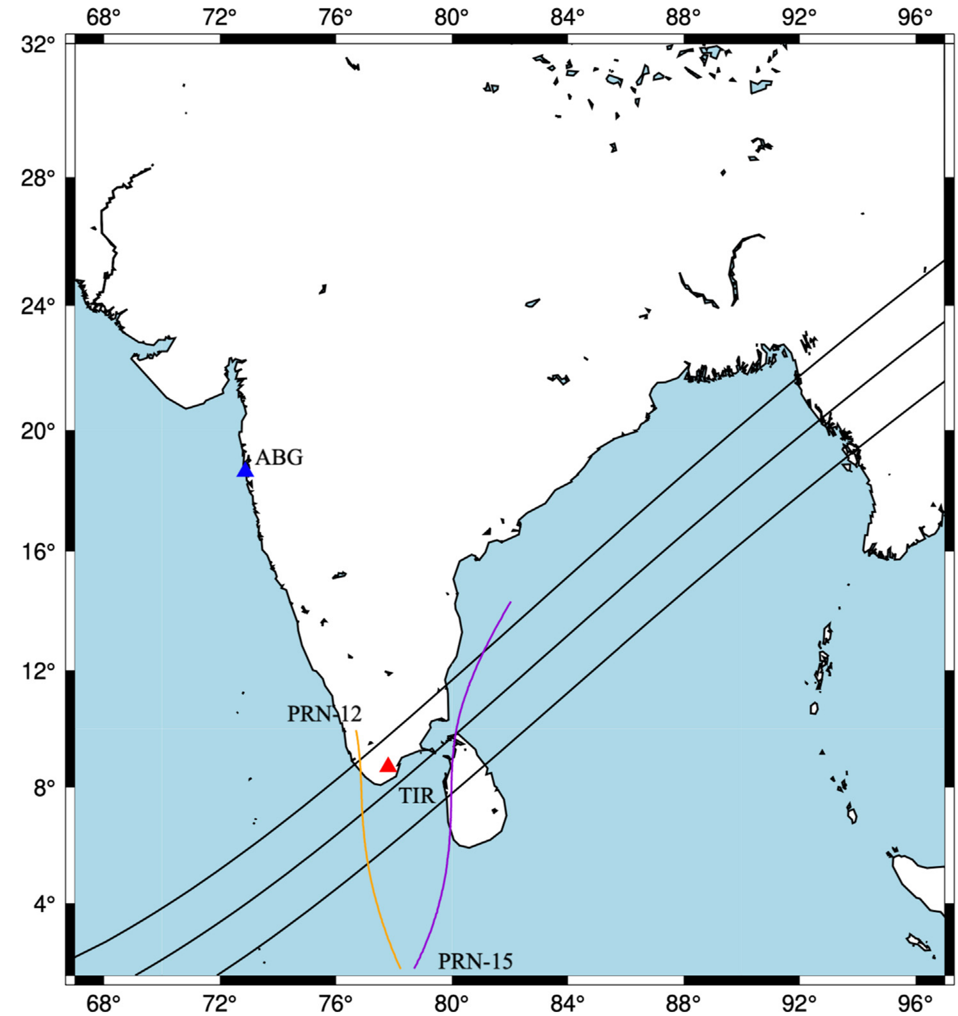

Fig. 1. Path of the 15 January 2010 solar eclipse over Indian region. The red triangle is the Tirunelveli station from which we have collected the ionosonde, GPS TEC, and geomagnetic data. The blue triangle represents the Alibag station from which we have collected the geomagnetic data to calculate the EEJ strength. Orange and dark violet curves are showing the path of PRN#12 and PRN#15 respectively.

angle represents the Alibag station from which we have collected the geomagnetic data to calculate the EEJ strength. Orange and dark violet curves are showing the path of PRN#12 and PRN#15 respectively. As Tirunelveli station falls under the maximum obscuration, several atmospheric/ionospheric/geomagnetic measurements were carried out simultaneously at the highest temporal resolutions to study the variability of the atmosphere/ionosphere system as well as sources of gravity waves and their propagation in the ionosphere during the passage of eclipse shadow. It can be seen that eclipse passed over southern India initially, while as time progressed the path of the eclipse had moved over the Bay of Bengal and later on into Bangladesh. Before further analysis of the eclipse event, we investigated the background conditions using solar, interplanetary, and geomagnetic measurements for any possible signatures of geomagnetic storms and any other solar events. It is found that all the background conditions remained steady and there is no evidence to suggest that eclipse day has geomagnetic/solar influence, and it shows geomagnetically quiet variations.

3. Observations

Here, we present important observations and analyses pertaining to the eclipse and control days to understand the similarities and differences for further examination.

3.1. Variability of F region on eclipse and control days using CADI ionosonde

Fig. 2 shows the diurnal variation of Range-Time–Frequency (RTF) between frequencies 2–8 MHz on (a) 14 January 2010, (b) 15 January 2010 (eclipse day), and (c) 16 January 2010 respectively to show a comprehensive picture of the reflected echoes on eclipse day and control days and their wave signatures in different regions of the ionosphere. While the x-axis shows the local time, the y-axis shows the virtual height. Three vertical lines designated as ‘B’, ‘M’, and ‘E’ in the figure on eclipse day indicate the ‘Begin’, ’Maximum’, and ‘End’ phases of the eclipse respectively. From the figure, it can be noticed that no upward/downward motion of the F1 layer at 11:00 LT

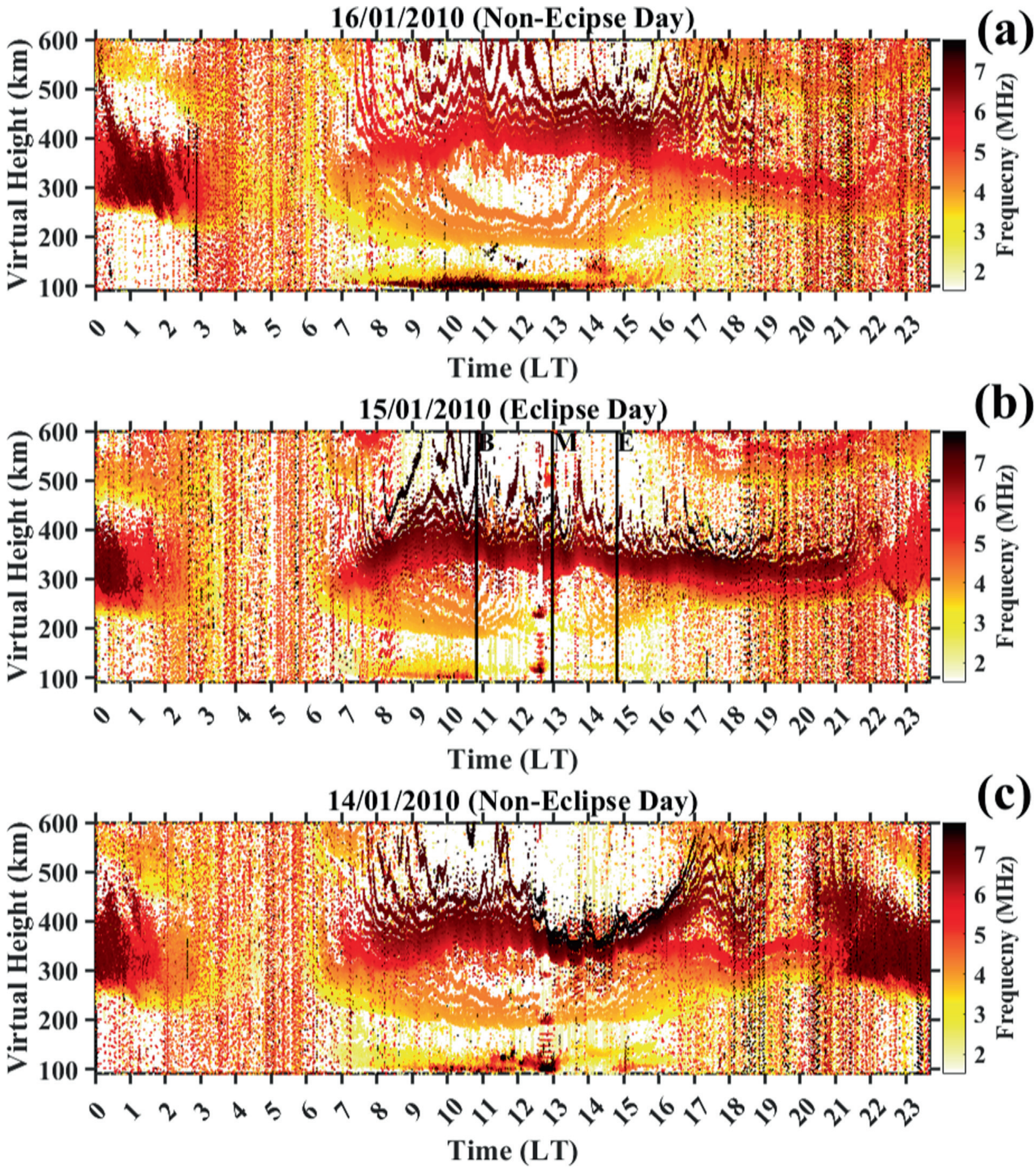

Fig. 2. Diurnal variation of Range-Time–Frequency (RTF) on eclipse and control days. Three vertical lines designated as 'B', 'M', and 'E' in the figure on eclipse day indicate the 'Begin', 'Maximum', and 'End' phases of the eclipse respectively.

can be seen on control days. However, an upward motion can be noticed on eclipse day in the beginning, while downward motion in the ending phase of the eclipse. Also, there are several small and large variations representing the eclipse-induced variations that can't be seen on other control days. In addition, the presence of a strong blanketing Es layer at the time of the eclipse can be noticed on 15 January 2010. Interestingly, we do notice short period density oscillations on 14 January 2010 at 7 MHz and above frequencies in the afternoon hours, unlike on other days. We also notice a strong spread F associated with enhanced PRE in the post-sunset hours on this day. This possibly may indicate the propagation of gravity waves from below and its seeding for the equatorial spread F that has been enhanced in the afternoon hours. However, such enhanced PRE and associated spread F have not been seen on the eclipse day suggesting that eclipse-induced gravity waves are mainly limited for a shorter duration. Fig. 3 displays the isoheight variations using real height data during 14 (bottom), 15 (middle), and 16 (top) January 2010. Note 'Blue', 'Red', and 'Green' colours indicate 14, 15, and 16 January 2010 respectively. Note that there are gaps in the Fig. 3(b, c) for 14 and 15 January 2010. This is due to the fact that strong Es layers are noticed from 12:34 to 12:58 LT and 12:34 to 12:46 LT on 14 and 15 January 2010 respectively. On the eclipse day, the strong Es layer is intensified at around 12:42 LT. These Esb layers almost masked the F layer movements and hence it is difficult to identify the variations. Here the analysis is performed by fixing the height (real) at every 5 km from 190–260 km and identifying the changes in the frequency. We extracted the isoheight variations at 2 min temporal resolution. From this analysis, it is possible to identify the altitude variation of eclipse-induced density variations on 15 January 2010 with reference to other control days. From the left side of the Fig. 3(b), it can be seen that reduction of density from 4.5 MHz to below 3.0 MHz which is nearly 33% in the lower altitudes on the eclipse day than on other control days. This density reduction is faster at lower altitudes than at higher altitudes. The response of the higher altitudes is slower and quickly returned to the normal levels. This reduction is mainly due to a sudden drop in ion/electron production in association with a faster recombination rate in the transition region from the E to F region. This suggests the transition of the photoionization process to the transport dominant process in the higher altitudes. To know more about the variations of the density on the eclipse event at different altitudes, further investigations were performed using isofrequency observations. Here, instead of height, we fixed the frequency to study the changes in the height (real). Fig. 4 displays the isofrequency variations during 14 (bottom), 15 (middle), and 16 (top) January 2010. Note 'Blue', 'Red', and 'Green' colours indicate 14, 15, and 16 January 2010 respectively. Here, the fixed frequencies are 4–6 MHz with an interval of 0.5 MHz. Note that there is no isofrequency observation from 12:34 to 12:46 LT on 15 January due to the presence of a strong Esb layer. Again, there are no isofrequency observations from 12:34 to 12:58 LT on 14 January due to the presence of the Esb layer. On eclipse day, the ionospheric F-layer started to move upward after the eclipse started. This height rise is not observed on control days. This is due to the decrease in ionisation during the eclipse period. To understand more about the eclipse effects

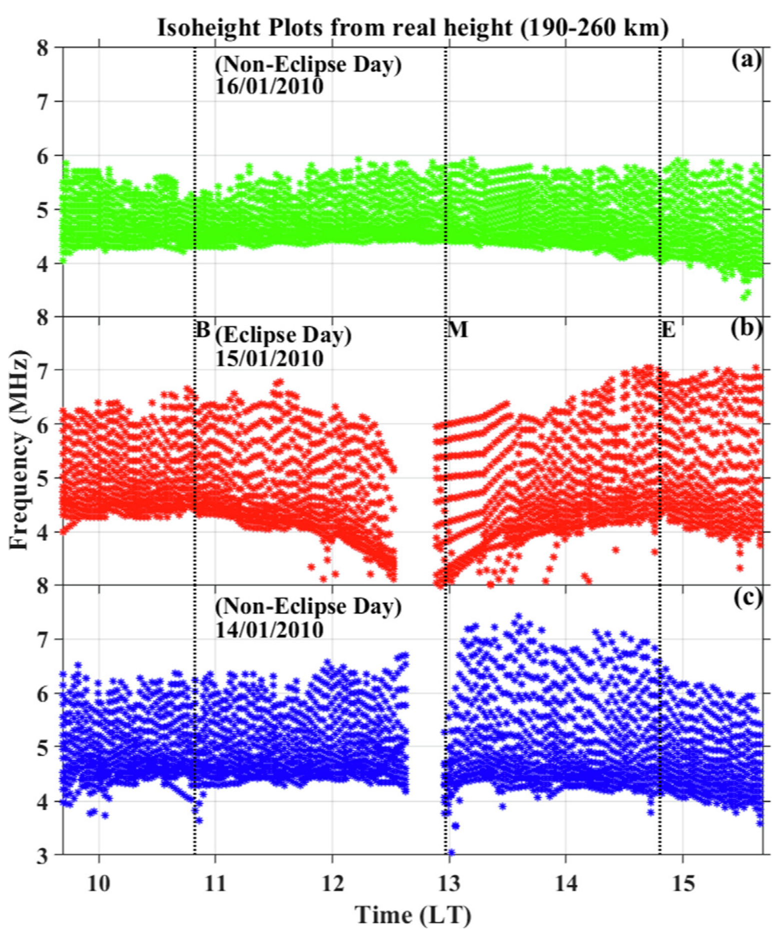

Fig. 3. Isoheight variations during 14 (bottom), 15 (middle), and 16 (top) January 2010. Note 'Blue', 'Red', and 'Green' colours indicate 14, 15, and 16 January 2010 respectively. The gap in the plotting on 14 and 15 January 2010 is due to the presence of strong Es layers.

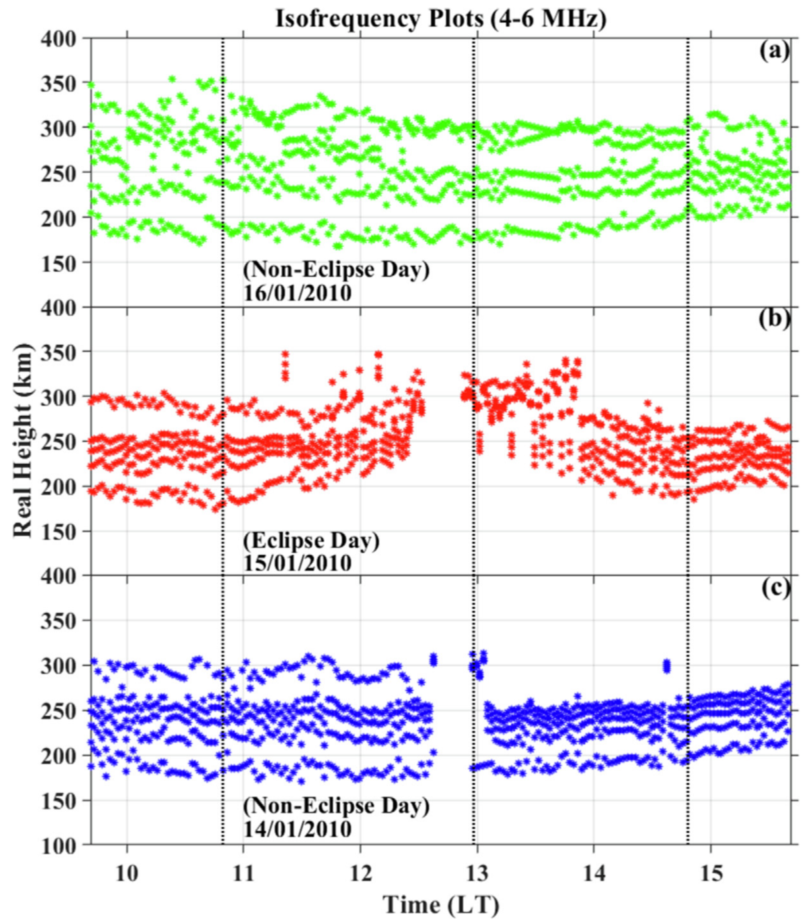

Fig. 4. Isofrequency variations during 14 (bottom), 15 (middle), and 16 (top) January 2010. Note 'Blue', 'Red', and 'Green' colours indicate 14, 15, and 16 January 2010 respectively. The gap in the plotting on 14 and 15 January 2010 is due to the presence of strong Es layers.

further investigations have been performed using FFT and wavelet analysis. The wavelet analysis has been performed using the method described in Torrence and Compo (1998). While FFT provides amplitude and phase of the wave, wavelet analysis, in addition, provides temporal evolution of the waves. These results are described in subsequent subsections.

3.2. Equatorial Electrojet (EEJ) strength variations

In order to study the variations in the E region currents on eclipse day, we investigated the EEJ strength over the Indian sector which is a proxy for the E region conductivity. The EEJ strength presented here has 1 min temporal resolution. The top panel of Fig. 5 shows the raw and filtered data of the temporal variation of EEJ strength over the Indian region on eclipse and control days. The middle and bottom panels of Fig. 5 show the temporal variation of fluctuations in EEJ strength on eclipse day using S-G filtering as used for ionosonde data and its wavelet analysis respectively. From the figure, it can be seen that the temporal variation of EEJ current on eclipse day is significantly different from that of the other control days where it is noticed that EEJ currents were reduced significantly even before the eclipse onset. St.-Maurice et al. (2011) have investigated the reason for the reduced EEJ currents prior to eclipse onset over Indian longitude. It is suggested that the travelling localized low pressure centre can result in a reduction of EEJ currents. The EEJ currents are reduced so much that they became negative known as CEJ currents. Since the current is proportional to the conductivity and drift velocity, the reduction in the EEJ current during the eclipse period could be related to both reduction of electron density and drift velocity that drives the current. From the figure, there is a strong fluctuation in EEJ just half an hour prior to eclipse onset. These fluctuations could be due to the passage of the eastern side of the low pressure centre that propagates ahead of the actual onset of eclipse (St.-Maurice et al., 2011). The wavelet analysis suggests that these EEJ fluctuations have a periodicity of ∼11–23 min that fall in the gravity wave spectrum.

3.3. Variability of the GPS TEC observations over Tirunelveli

Now in order to investigate further the eclipse-driven disturbances in the TEC, we present GPS TEC observations over Tirunelveli on eclipse day and control days.

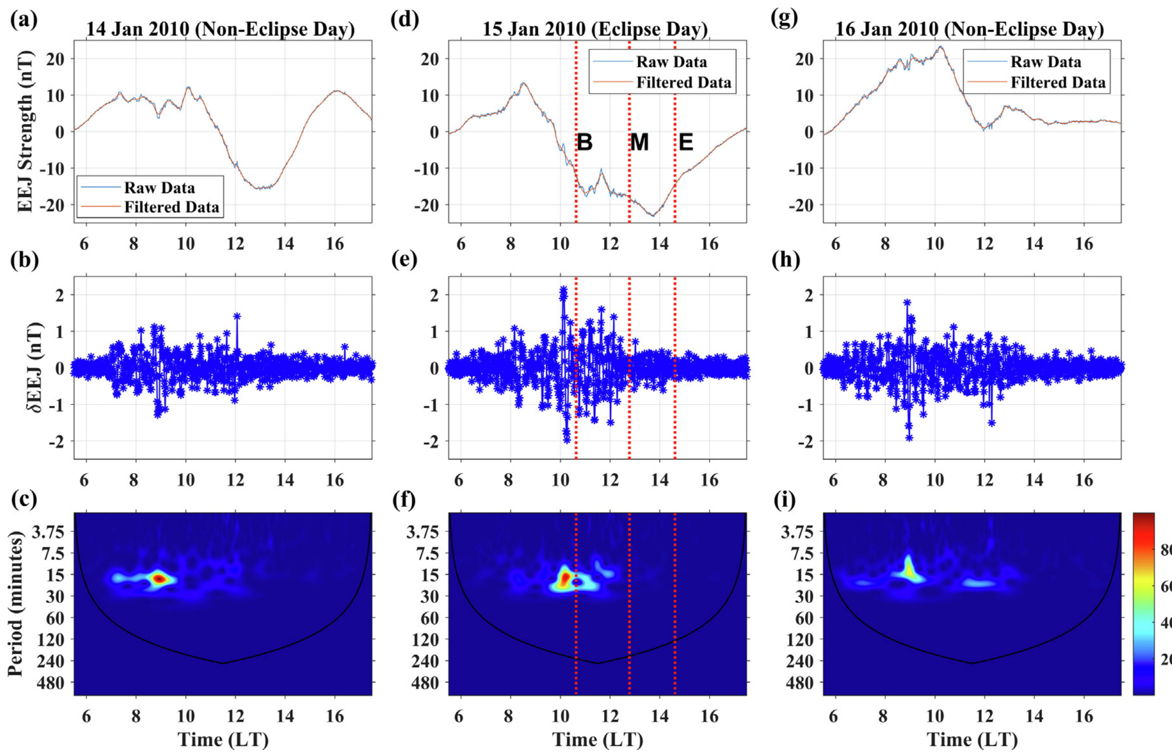

Fig. 5. Temporal variation of equatorial electrojet (EEJ) strength on eclipse and control days (top panel), temporal variation of fluctuations in EEJ strength on eclipse and control days using S-G filtering (middle panel), and its wavelet analysis (bottom panel).

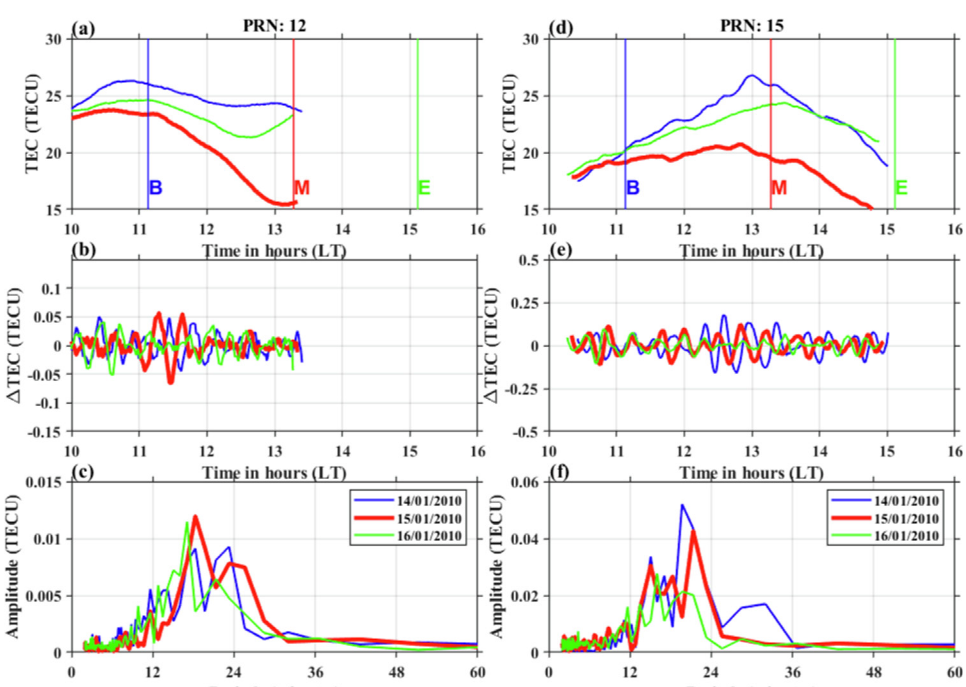

Fig. 6. Temporal variation of vTEC on eclipse day and control days for (a) PRN#12 and (d) PRN#15 (top panel), their S-G filtered TEC fluctuations (middle panel), and FFT analysis of the fluctuations (bottom panel).

Since the path of PRN#12 and PRN#15 is very close to the maximum eclipse shadow region, we utilized them to study the density reduction and also to see gravity wave-like oscillations. Now we present the TEC, S-G filtered TEC fluctuations, and their FFT analysis using both PRN#12 and PRN#15 in Fig. 6 on eclipse day and control days to identify the eclipse-induced density reduction and wave-like fluctuations in TEC. From the figure, it can be noticed that TEC on the eclipse day is significantly reduced in both PRN#12 and PRN#15, but the ΔTEC as presented in Fig. 6(c,d) showed higher ΔTEC fluctuations on PRN#12 but not on PRN#15. This could be due to different satellite paths. This could also be due to the weak impact of the eclipse on peak density as compared to the F1 layer that we notice. The FFT analysis on the eclipse day and control days for PRN#12 and PRN#15 showed gravity wave periodicities. While gravity wave activity is evident on the eclipse day in PRN#12 and PRN#15, interestingly, we do see the presence of gravity waves on other control days as well. But it is seen that multiple dominant periods (18–21 min) were present simultaneously on eclipse day having periods in the frequency band of gravity waves. However, it is not evident whether the frequencies that were seen in our observations were excited in the lower atmosphere or in situ generated in the ionosphere. This aspect is examined using group and phase velocity.

3.4. Altitude variation of phase velocity and group velocity

Till now, we have performed various periodogram analyses to investigate different types of waves and their corresponding amplitudes and periods. But we didn't investigate the sources for the occurrence of these waves. As mentioned in the introduction, the gravity waves, bow waves, and acoustic waves are known to be excited during eclipse events due to sudden cooling/heating and reduction of photoionization. In this investigation, we are mainly focusing on the wave oscillations that are in the range of gravity waves. Also, as we didn't have enough knowledge about the altitude variation of these waves, we investigated the altitude variation of these waves and their propagation. Using the altitude variation of waves, we estimated the wave parameters namely wave phase velocity and group velocity, and their altitude variation. Using the altitude variation of group and phase velocity, it is possible to identify whether these waves are generated through in situ sources or propagated from below for gravity waves. It may be mentioned that such a technique has been used earlier to estimate the phase velocity and group velocity. According to this method, the group velocity is the mean flow velocity of several waves whereas phase velocity is the flow of a single dominant wave.

3.4.1. The procedure of extracting group and phase velocities

We mainly use isoheight to estimate the group and phase velocities as described in (Liu et al., 1998; Altadill et al., 2001b). The isoheight data as obtained using real height analysis has been subjected to FFT analysis at each height to obtain phase and group velocities. We have assumed the time series of plasma frequency at different heights (real) as

$$p_i = p_o + \sum_{j=1}^{N/2} (M_j \cos \sigma_j t_i + N_j \sin \sigma_j t_i) \tag{1}$$

where p_i are representing time series of plasma frequencies at different real heights.

If the plasma frequency oscillations are caused by gravity waves, it is possible to write them as the combination of plane wave fluctuations as follows:

$$p_i = p_o + \sum_{j=1}^{N/2} S_j \cos(\sigma_j t_i - k_i x - l_i y - n_i z) \tag{2}$$

σ_j=frequency of jth harmonic and k_i, l_i, and n_i are x, y, and z component of wavenumbers respectively.

Usually, the ionosonde is operated in the vertical sounding mode for routine observations. In the case of AGW studies, the horizontal wavelength is greater than the horizontal range of ionosonde. As a result of which the horizontal components of observed targets do not change along the ionosonde beam. Hence the remaining component i.e., the vertical component is useful for the group and phase velocity analysis (Liu et al., 1998). Assuming the x and y are horizontal components and z is the vertical component, we can write the phase of the plane wave as

$$n_i z = \tan^{-1}\left(\frac{N_j}{M_j}\right) = \phi_j(z) \tag{3}$$

From Eq. 3, the vertical wavenumber can be calculated by differentiating the phase $\phi_j(z)$ with respect to z.

$$n_i = \frac{d\phi_j(z)}{dz} = \frac{d\left(\tan^{-1}\left(\frac{N_j}{M_j}\right)\right)}{dz} \tag{4}$$

Further, the vertical phase velocity can be calculated as follows

$$v_{phase} = \frac{\sigma_j}{n_i} \tag{5}$$

In order to calculate the group velocity, we considered the propagation of the wave packet. The velocity with which energy is transmitted is referred to as group velocity. The vertical group velocity can be calculated by using the following formula

$$v_{group} = \frac{d\sigma}{dn} \tag{6}$$

FFT analysis of data gives amplitudes and phases. The harmonic corresponding to maximum amplitude is used to estimation of phase velocity. On the other hand, the group velocity is estimated by considering the harmonics closely distributed around the maximum amplitude having a probability of existence of 95% or above.

In our case, after performing the S-G filtering to the isoheight data, the filtered data containing the density perturbations (Δ density) are subjected to FFT for several altitudes. We have applied the FFT only when the growth phase of the eclipse is dominant. The main idea is to study the generation of wave activity in the atmosphere–ionosphere system during the passage of the solar eclipse. The data gap in the isoheight plot is due to the presence of a

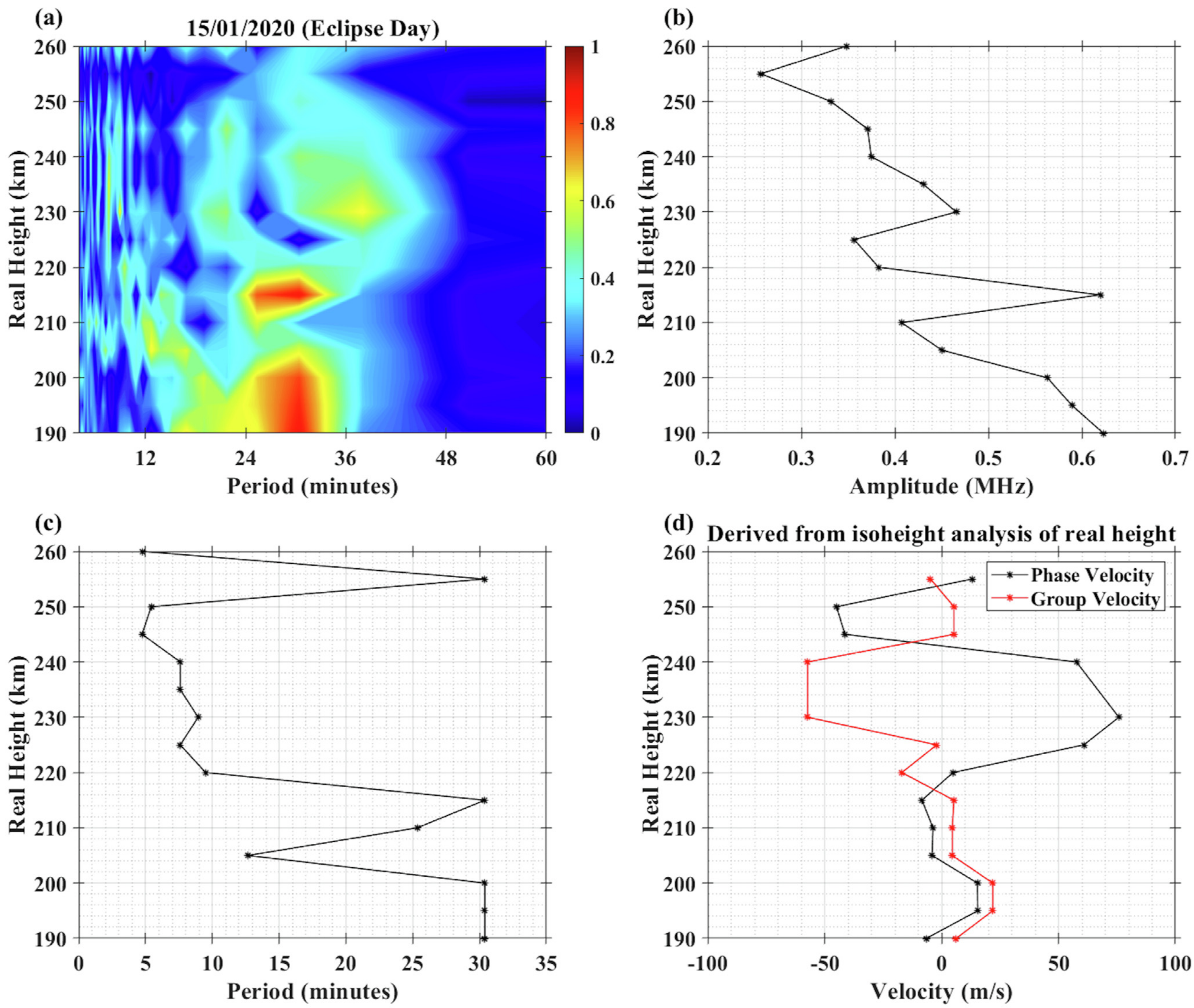

Fig. 7. Altitude variation of (a) amplitude after FFT analysis on isoheight variations, (b, c) peak amplitude and corresponding periods, and (d) group and phase velocity of the gravity wave in isoheight variations for eclipse day.

strong Es layer and hence has been avoided while estimating altitude variation of wave periods using FFT analysis as we considered the data points falling under only the growth phase.

Fig. 7(a) shows the contour map of the altitude variation of wave amplitude as a function of frequency (period) using FFT analysis on all the isoheight on the eclipse day. The amplitude scale of the variations is normalized to the maximum amplitude. The amplitude variation is relatively higher in the bottom side of the F-layer from 190–220 km altitude for the waves having periods in the range of 24–36 min. But one can see amplitude is less beyond 220 km altitude. Fig. 7(b,c) show the altitude variation of peak amplitude and corresponding periods respectively. As one moves upward with altitude, peak amplitude starts to decrease from 0.63 MHz to 0.3 MHz. In the lower altitudes from 190–220 km the periods corresponding to peak amplitude vary from 12–30 min whereas in the higher altitudes i.e. beyond 220 km periods are small and vary from 5–10 min.

Fig. 7(d) shows the altitude variation of the group and phase velocity derived from isoheight analysis. In Fig. 7(d), the black line with an asterisk represents phase velocity, whereas the redline with an asterisk indicates group velocity. It can be noted that the wave structures seen at different heights starting from 190 km to 260 km are not of one type. The dominant waves are found in the band of 24 to 36 min. It is possible that the sources for these waves could be different. To identify the source of such wave structures, we performed phase and group velocity analysis where we considered the dominant periods between 24 to 36 min. The results show that in the lower altitudes the phase velocity is upward up to 205 km and then it is downward up to 215 km. The group velocity is upward up to 215 km. The upward propagating group velocity and the downward propagating phase velocity indicate the upward propagating gravity waves from the bottom. However, it can be seen that below 220 km, the group and phase velocity are not showing any counter propagation. As this region is the bottom side of the F-region (F1-Layer) where the recombination is faster as compared to the upper altitudes (>220 km), the wave-like structure as seen here merely represents the large-scale density depletion (see Fig. 3)) and may not be showing the gravity wave characteristics. The region below 220 km is a region of complex coupling of not only background electrodynamics but also neutral as well as chemical dynamics which may play an important role in the case of gravity wave propagation. The cooling/heating processes during this solar eclipse due to the decrease and increase of solar ionizing radiation may result in the change of the scale height of the plasma and neutrals. This in turn results in the downward and upward motion of the plasma and neutrals. Hence, in addition to the propagating gravity waves, these upward and downward motions can also add additional disturbances. As a result, it is hard to distinguish the AGW in the altitude range of 190–210 km. This could be one of the reasons why the wave structures in the altitude range of 190–210 km are not showing the property of AGW. But 220 km onwards the wave-like structures are showing the property of gravity waves which may be due to the enhanced gravity wave amplitudes that might have suppressed other wave disturbances. An important property of gravity waves is that the phase propagates downward while the wave is moving upward or vice versa. Beyond 220 km, it is also observed that the phase velocity is oscillating from downward to upward and then upward to downward. But group velocity is oscillating between upward to downward and then downward to upward. This counter propagation of vertical group and phase velocity indicates the excitation of gravity waves in the lower altitudes. Hence, it is possible that the sources of these gravity waves could be located in the lower altitudes. Previous studies by Liu et al. (1998), Altadill et al. (2001b) showed that the source of atmospheric gravity waves is situated between 176–195 km and 200–220 km during different solar eclipses respectively. However, based on the results obtained from this event, we could not identify the in situ generation of gravity waves. In addition, it is noticed that the EEJ strength showed the dominance of 25 min periodicity prior to the eclipse onset and continued after the eclipse onset. Many other results obtained from the lower atmosphere and MLT region do suggest the presence of gravity wave-like oscillations at the time of the eclipse (Taori et al., 2010; Dutta et al., 2011; Manju et al., 2014). Accordingly, we also examined gravity wave sources in the D region which will be discussed next.

3.5. D region density (fmin) variability

In order to obtain a clear picture of the gravity wave propagation and its source during eclipse passage over Tirunelveli, we have scaled the lowest observed frequency in the ionogram (fmin) on eclipse (15 January 2010) and control days (14 January 2010 and 16 January 2010). Fig. 8 shows (top panel) temporal variation of raw and filtered fmin, (middle panel) temporal variation of fluctuation in fmin, and (bottom panel) wavelet analysis of fluctuations

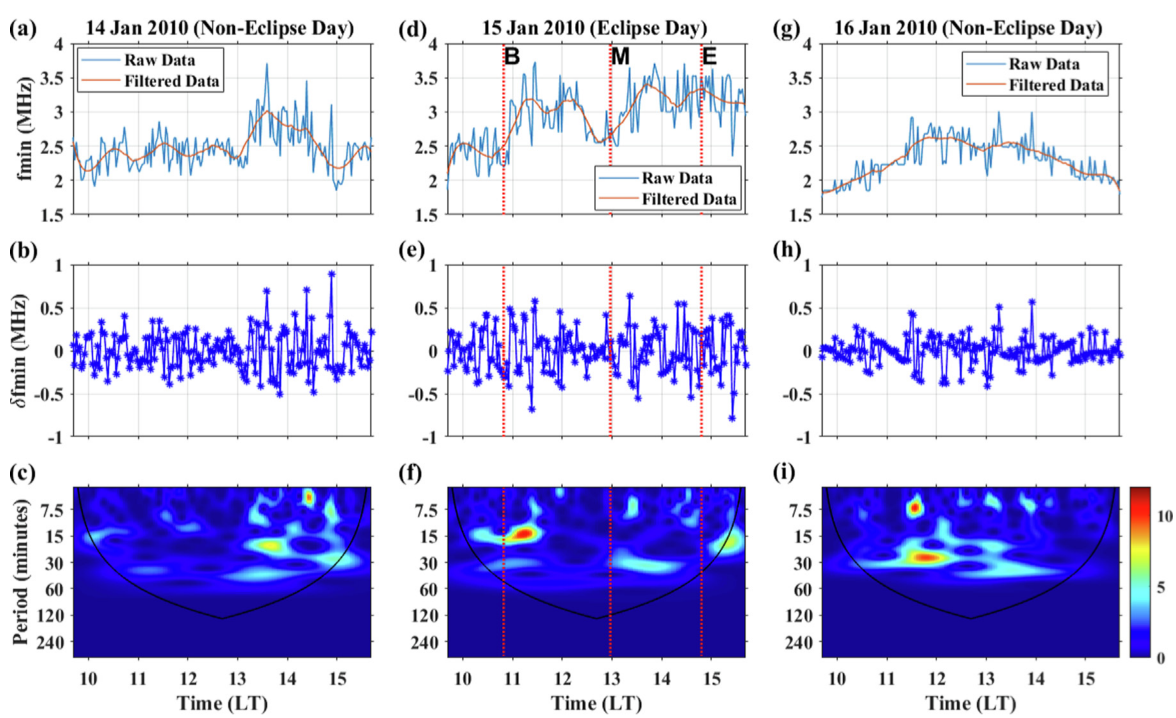

Fig. 8. Temporal variation of raw and filtered fmin (top panel), temporal variation of fluctuations in fmin (middle panel), and wavelet analysis of fluctuations in fmin (bottom panel) for 14, 15, and 16 January 2010 respectively.

in fmin for 14, 15, and 16 January 2010 respectively. From these figures, we can clearly see that the temporal variation fmin shows unusual variations on the eclipse day as compared to the control days. The fmin has been used as a proxy for D-region ionization and hence it is expected that the D-region density should decrease during the eclipse period. But compared to control days the fmin values are significantly high. This may be due to the downward drift motion of ionization from the top. As the eclipse started, the fmin value for the eclipse day shows an increasing trend as compared to both the control days. The eclipse day fmin value started to decrease during the maximum phase and reached close to control day values. After the maximum phase of the eclipse, the fmin values show an increasing trend for both control and eclipse days. These unusual variations in fmin may be due to the perturbations in the lower ionosphere caused by eclipsed induced wave activity. Further, the wavelet analysis of fluctuations in fmin values indicates the presence of gravity of like oscillations on the eclipse and control days. During the beginning phase of the eclipse, the amplitude is slightly higher as compared to the control days. We believe these wave-like oscillations of period ∼11–22 min in the D-region of the ionosphere are mainly caused due to the eclipse-induced changes in the lower/middle atmosphere. In the previous section, we have shown that there is no evidence of in situ generated gravity wave oscillations. However, the simultaneous presence of wave-like oscillations in EEJ strength and fmin values can be regarded as proof of the generation of gravity waves in the lower/middle atmosphere and propagating above.

3.6. COSMIC Electron density profiles

Fig. 9 shows the (a) electron density profiles as obtained from the COSMIC on 15 (eclipse day), and 14 and 16 (control days) January 2010 and (b) the S-G filtered altitude density variations (Δ density) on these days. From the figure, it can be noticed that clean evidence of a reduction of electron density on eclipse day than on control days with the presence of strong density fluctuations on eclipse day. The vertical wavelength of these waves is found to be ∼50 km. It may be noted that though the density fluctuations are seen on control days, higher density fluctuations are seen in the F1 layer on the eclipse day than on control days. From this, we can say that the density profiles are highly disturbed on eclipse day and their amplitudes are significantly higher in the lower ionosphere than in the topside ionosphere.

4. Discussion

Gravity waves are known to transport energy and momentum from the source region to the ionospheric heights. These gravity waves can be generated at different altitudes depending upon their sources (convection, wind shears, and orography) in the atmosphere–ionosphere

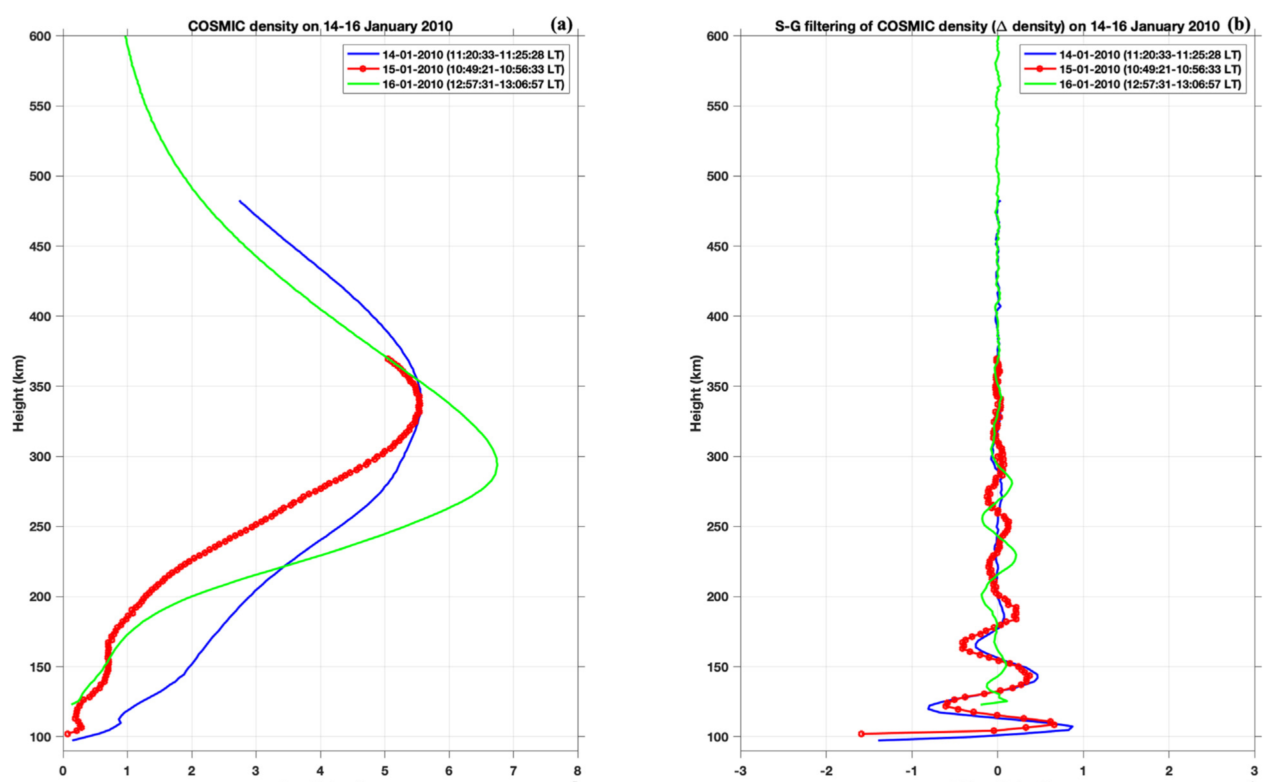

Fig. 9. (a) Altitude variation of cosmic electron density profiles and (b) altitude variation of density fluctuations (Δ density) on 14–16 January 2010 over Tirunelveli.

system. In addition, solar eclipses are one of the unique natural phenomena that can also generate gravity waves. Numerous attempts have been made in the past to study the characteristics and source mechanism of gravity waves generated during eclipses. Although gravity waves are always present in the atmosphere–ionosphere system, sudden change in the incoming solar radiation can provide a chance to identify the sources of gravity waves excited during a solar eclipse. While several studies have been made in the past on eclipse-induced gravity waves using the 15 January 2010 eclipse over India, however, there is no clear evidence that has emerged to show the source location of these gravity waves during the passage of the eclipse. In addition, unlike past studies, in this study, we have utilized the control days to show the differences in variability between eclipse and control days. While some studies have suggested that they are propagating from the below atmosphere, other studies suggest that they are generated in situ in the ionosphere. Some studies have also mentioned that they have noticed both propagating from below as well as from above. In this study, an attempt has been made to study the altitude variation of short-period gravity waves using altitude variation of density perturbations, their dominant periods, vertical group and phase velocities, and their propagation directions. In this method, we are targeting different height bins from 190 km to 260 km to identify the source location of gravity waves taking density fluctuation at each height bin where gravity waves within a band of ~5–50 min periodicity are observed. Since the solar eclipse occurred on a geomagnetically quiet day, there is no influence of wave activity from the auroral zone expected. In addition, on the eclipse day, there was no extreme meteorological event to generate enhanced gravity wave activity. Therefore, the observed gravity waves with enhanced amplitude on the eclipse day are due to eclipse-driven changes in the atmosphere–ionosphere system. The main aim of this work is to locate the source of these gravity waves. The gravity wave oscillations observed in the ionospheric plasma are showing numerous wave packets propagating in the ionosphere during the eclipse period. The unique variations in amplitude and period of gravity wave fluctuations are mainly due to the fact that we are taking a wide band of gravity waves which could be generated at different altitudes due to the perturbation in the atmosphere–ionosphere system caused by the solar eclipse. The wave parameters are derived using the Fourier transform which is leading to the mixing of information in time. Hence, the wave propagation parameters measured at a particular frequency can essentially result from the contributions of different waves corresponding to the same observed frequency but with different time stamps. Šauli et al. (2007) have used wavelet analysis to get the joint information of time and frequency of gravity wave fluctuations whereas we have used FFT to obtain the wave parameters of the gravity wave fluctuations. The altitude variations of gravity wave fluctuations are further used to identify the source location of these waves by calculating vertical phase and group velocity. Vertical phase and group velocity are showing opposite trends which further indicates the propagation of gravity waves from the lower ionosphere. In addition, based on the results and analysis as shown in the previous section, we do find that eclipse on 15 January 2010 has impacted the densities in the D, E, and F1 regions significantly due to sudden changes in the production, loss, and transport processes due to sudden decrease of ionization over southern India. However, no such reduction has been noticed in the F2 layer. Further, combining all the gravity wave oscillations observed in EEJ, fmin, and ishoheight data, we can suggest the consistent presence of gravity waves at different ionospheric altitudes. As this eclipse passage was noticed close to the magnetic equator at local noon hours, it also produced unique electrodynamics over Indian longitude(St.-Maurice et al., 2011; Choudhary et al., 2011). The eclipse caused a sudden drop in the ionization that affected both E and lower F regions of the ionosphere as also can be seen in our observations. It is believed that this triggered additional electrodynamics due to the development of a sudden low pressure system that moved east with the Moon's shadow. St.-Maurice et al. (2011) suggested that significant electrodynamics is believed to be developed over the Indian sector on this eclipse day. They suggested that the eclipse has produced a counter Sq current and a counter electrojet system that quickly moved eastward as the shadow moved and E region currents were also interrupted due to a decrease in E region conductivity at the centre of the low pressure system that caused temporary PRE. The reduction of TEC over the crest region at the time of the eclipse is also believed to be due to the reduced drifts (Choudhary et al., 2011). In addition, our observations at Tirunelveli also showed a rise in the isoheights during the initial phase of the eclipse but a fall in the real height in the recovery phase. However, due to the presence of strong blanketing Es layers, we couldn't notice anything for a brief period in the main phase of the eclipse. Across this rise and fall, there exists a strong density gradient in the upper E and lower F region that is believed to be triggering sources for excitation of 150 km echoes in the radar observations over Gadanki (Patra et al., 2011). Adeniyi et al. (2007) have investigated the variations in the electron density in the E, F1, and F2 regions over the equatorial region in the African sector due to the 29 March 2006 eclipse event and noticed the presence of drastic reduction in the E and F1 layer density without much delay but there is a lag of 1 h 20 min or more to notice reduction in the F2 layer density. They also observed a major departure of hmF2 from the normal day variations. However, interestingly, no gravity wave-type oscillations have been reported by them, unlike the present investigations where we noticed the presence of gravity wave-type oscillations.

Nayak et al. (2012) have suggested that there is a reduction in the density of foF1. The results presented in the previous section do suggest that there is a reduction of density in the F1 layer and lower F region whereas no such decrease of h'F1 was noticed. However, they didn't study the gravity wave perturbations and their source location that we have investigated in the present analysis. Our results presented in the previous section showed evidence of higher amplitude gravity waves on the eclipse day than on control days. Interestingly, we also notice the weak presence of gravity waves on other control days which we believe could be due to lower atmospheric processes. Most of the investigations were revolving around the idea that these waves were excited at the surface or in the stratosphere where it is believed that sudden cooling and heating could excite atmospheric gravity waves. Initially, this idea was proposed by Chimonas and Hines (1970) which was verified by Davis and Da Rosa (1970) using radio experiments. But few studies suggest that the gravity waves as seen in the ionosphere could be due to sudden cooling of the ionosphere itself (Altadill et al., 2001a). Beer (1973), on the other hand, has suggested that the sources for these gravity waves could be in the regions of molecular oxygen above 90 km, the ozone layer at 50 km that absorb solar UV radiation, and the surface/ground and tropospheric altitude where carbon dioxide and water vapour can absorb the energy and re-radiate from the surface due to solar eclipses. Accordingly, several campaigns have been conducted at several locations during eclipse events to verify that the gravity waves as seen in the ionosphere are indeed propagated from the surface or in situ (Liu et al., 1998; Altadill et al., 2001b; Manju et al., 2014). The acoustic and gravity wave characteristics as investigated based on the application of wavelet amplitude and phase spectra on the high resolution ionosonde observations during the 11 August 1999 eclipse event do suggest that the gravity waves could be propagated from the F1/F2 transition region as well as abrupt modifications in the ozone heating and cooling in the stratosphere (Šauli et al., 2007). In the present study, we have noticed the presence of gravity wave-type oscillations with higher amplitude in the lower F layer based on isoheight analysis. In addition, the altitude variation of eclipse-induced wave activity using the isoheight analysis does suggest the presence of eclipse-induced wave perturbations that are different from the control day variations. The GPS TEC over Tirunelveli and its wave analysis also suggest that there is a prolonged gravity wave type of oscillations during the eclipse day than on other control days.

Periodogram analysis using wavelet and FFT analysis suggests that these wave periods could be associated with the gravity wave periods. Our results also showed a reduction of TEC that is below normal levels and the presence of CEJ that is opposite to normal currents over the Indian region during the passage of the Annular Solar Eclipse in India. But we do notice gravity waves in TEC observations on control days which could be due to regular gravity waves. However, the gravity waves on the eclipse day were found to be more prolonged than on other days. It is known that eclipse-induced strong lunar tidal forces are also dominated during eclipses and can possibly produce counter electrojet (Vyas and Sunda, 2012; Panda et al., 2015). The presence of gravity wave-like oscillations with periods in the range of 20–90 min have also been noticed in the GPS TEC observations in the path of totality and away from the totality during the Great American Eclipse on 21 August 2017 (Nayak and Yigit, 2018). However, their observations also suggest that the gravity wave amplitudes are higher at the locations that are closer to the totality than away from the totality. Based on the altitude variation of group and phase velocities as obtained from the isoheight analysis in the present study, we suggest that these waves were propagating from the below atmosphere and there is no clear evidence for excitation of in situ gravity waves in the ionosphere. These results are in contrast to those seen by Liu et al. (1998) and Altadill et al. (2001b). Altadill et al. (2001b) have suggested that since the transition region between E and F region is significantly affected by the photoionization and dynamics, it is possible that this region could be prone to more turbulence and can produce gravity wave oscillations. Since we noticed strong Es layers, the presence of turbulent structures and gravity waves in the F layer could not be recorded in ionosonde. Since Es layers are excited by strong winds and wind shears which are possible during eclipse and CEJ events, the presence of strong Es layers in our case does support that there were strong winds and wind shears with altitude over the equatorial region due to sudden local cooling of the atmosphere/ionosphere.

Taori et al. (2010) have investigated the middle atmospheric dynamics using winds from medium frequency (MF) radar and temperature from TIMED-SABER satellite observations during this eclipse over Tirunelveli and suggested that not only background mean zonal winds are reduced significantly but also mesospheric temperature inversion layers are noticed on eclipse day than on control days that may assist gravity waves to propagate to higher altitudes. Their results also showed that there is a higher amplitude gravity wave on eclipse day than on other control days which supports our findings of higher amplitude gravity waves in the isoheight analysis. We have also examined the SABER temperature data during this period where we do notice strong inversion layers or temperature gradients in the MLT region that may excite gravity waves (not shown here). Also, Dutta et al. (2011) suggested that the tropical troposphere-stratosphere exhibited a reduction of temperature and strong fluctuations in the zonal winds having high frequency gravity waves during this eclipse day than on control days at Gadanki and Hyderabad. These results suggest that there is a strong possibility that gravity waves can indeed be propagated from the lower atmosphere. This result is in confirmation with our observations of fmin and EEJ strength that are showing gravity wave signatures.

To understand further our results and their relevance to studies made in the past, we have compared our results to that of digisonde observations at Trivandrum as it is closer to our station (∼100–120 km) and this station is also on the path of the passage of moon's shadow. In addition, rocket observations were utilized in their observations to measure the neutral winds. Their results also suggest that they noticed atmospheric gravity waves in both ionosonde and neutral wind measurements. But they suggested that these gravity waves could have been excited in situ in the F1 layer and could have been propagated to the lower and upper altitudes. Due to the spatial separation of nearly 100–120 km between Trivandrum and Tirunelveli stations, it is possible that we may be experiencing the waves arising from the lower atmosphere due to their dominance over in situ generated gravity waves. While the results presented here suggest that gravity waves could have been excited in the lower/middle atmospheric sources during eclipse passage, we believe that more studies are still needed along with neutral winds observations to identify the sources of eclipse-driven gravity waves. In the future, we wish to address this issue in great detail using both observation and modelling studies.

5. Summary and conclusions

We have investigated the variability of the equatorial ionosphere on the 15 January 2010 Annular Solar Eclipse along with two control days to study the eclipse-induced altitude variation of gravity waves and their source location in addition to density reduction and density perturbations using high resolution (2 min) ground based observations of ionosonde, GPS TEC, and EEJ strength over Tirunelveli. In addition, we also utilized COSMIC density profiles on eclipse and control days. The real height analysis has been performed to obtain isoheight/isofrequency variations. We performed periodogram analysis on isoheight/isofrequency during the eclipse and control days to study the altitude variation of the density fluctuations, gravity waves, and their propagation. The important results are summarised as follows:

1. The results using isoheight analysis indicate a reduction of ~33% in the lower ionosphere whereas no change has been noticed close to the F layer peak on the eclipse day.
2. The periodogram analysis on isoheights using real height data further indicates the presence of gravity waves with dominant periods in the range of 5–30 min.
3. The altitude variation of estimated group and phase velocities showed opposite trends suggesting that the sources of these gravity waves are from below.
4. The results further showed higher amplitude gravity waves in the fmin, TEC, and EEJ strength on the eclipse day than on control days.
5. The presence of gravity waves in fmin, EEJ strength, and isoheights (real heights) suggest their possible excitation from the below atmosphere on the eclipse day.
6. COSMIC density profiles showed evidence of enhanced gravity wave activity having a vertical wavelength of ~50 km in the lower ionosphere on eclipse day than on control days.

Declaration of Competing Interest

The authors declare that they have no known competing financial interests or personal relationships that could have appeared to influence the work reported in this paper.

Acknowledgments

The work presented in this paper is through financial support from the institute project 'NECLAS'. We are thankful to the Director, IIG for his kind support and necessary help. We also wish to thank the late Dr. Diwakar Tiwari, IIG for conducting the eclipse field campaign at Tirunelveli to collect high resolution ionosonde measurements and make the data available for the investigations presented here. We are also thankful to Mr. Selvaraj and Mr. Emperumal, both technical officers, at Tirunelveli for providing the necessary technical help in carrying out this experiment without which we couldn't have had this campaign successful. We also wish to thank Dr. Keith Groves, Boston College, USA for providing the SCINDA GPS receiver and its data for the studies presented here. We are thankful to the technical staff of the geomagnetic data collection and processing group at IIG for providing us with the EEJ strength data for the studies presented here. COSMIC electron density profile data presented here are obtained from https://www.cosmic.ucar.edu/.

References

Adeniyi, J.O., Radiceila, S.M., Adimula, I.A., et al., 2007. Signature of the 29 March 2006 eclipse on the ionosphere over an equatorial station. J. Geophys. Res.: Space Phys. 112, A06314. https://doi.org/10.1029/2006JA012197.

Altadill, D., Gauthier, F., Vila, P., et al., 2001a. The 11.08.1999 solar eclipse and the ionosphere: a search for the distant bow-wave. J. Geophys. Res.: Space Phys. 63 (9), 925–930. https://doi.org/10.1016/S1364-6826(00)00204-2.

Altadill, D., Solé, J.G., Apostolov, E.M., 2001b. Vertical structure of a gravity wave like oscillation in the ionosphere generated by the solar eclipse of august 11, 1999. J. Geophys. Res.: Space Phys. 106 (A10), 21419–21428. https://doi.org/10.1029/2001JA900069.

Bamford, R.A., 2001. The effect of the 1999 total solar eclipse on the ionosphere. Phys. Chem. Earth, Part C: Solar, Terrestrial Planet. Sci. 26 (5), 373–377. https://doi.org/10.1016/S1464-1917(01)00016-2.

Beer, T., 1973. Supersonic generation of atmospheric waves. Nature 242 (5392), 34. https://doi.org/10.1038/242034a0.

Chimonas, G., Hines, C.O., 1970. Atmospheric gravity waves induced by a solar eclipse. J. Geophys. Res. 75 (4), 875. https://doi.org/10.1029/JA075i004p00875.

Chimonas, G., Hines, C.O., 1971. Atmospheric gravity waves induced by a solar eclipse, 2. J. Geophys. Res. 76 (28), 7003–7005. https://doi.org/10.1029/JA076i028p07003.

Choudhary, R.K., St.-Maurice, J.P., Ambili, K.M., et al., 2011. The impact of the january 15, 2010, annular solar eclipse on the equatorial and low latitude ionospheric densities. J. Geophys. Res.: Space Phys. 116, A09309. https://doi.org/10.1029/2011JA016504.

Davis, M.J., Da Rosa, A.V., 1970. Possible detection of atmospheric gravity waves generated by the solar eclipse. Nature 226 (5251), 1123. https://doi.org/10.1038/2261123a0.

Dutta, G., Vinay Kumar, P., Venkat Ratnam, M., et al., 2011. Response of tropical lower atmosphere to annular solar eclipse of 15 january,

2010. J. Atmos. Solar Terr. Phys. 73 (13), 1907–1914. https://doi.org/10.1016/j.jastp.2011.04.025.

Evans, J.V., 1965a. An f region eclipse. J. Geophys. Res. 70 (1), 131–142. https://doi.org/10.1029/JZ070i001p00131.

Evans, J.V., 1965b. On the behavior of f 0 f 2 during solar eclipses. J. Geophys. Res. 70 (3), 733–738. https://doi.org/10.1029/JZ070i003p00733.

Fritts, D.C., Luo, Zhang, 1993. Gravity wave forcing in the middle atmosphere due to reduced ozone heating during a solar eclipse. J. Geophys. Res. 98 (D2), 3011–3021. https://doi.org/10.1029/92JD02391.

Jakowski, N., Stankov, S.M., Wilken, V., et al., 2008. Ionospheric behavior over europe during the solar eclipse of 3 october 2005. J. Atmos. Solar Terr. Phys. 70 (6), 836–853. https://doi.org/10.1016/j.jastp.2007.02.016.

Koucka´ Kni´žova´, P., Mosňa, Z., 2011. Acoustic-Gravity Waves in the Ionosphere During Solar Eclipse Events. IntechOpen. https://doi.org/10.5772/19722.

Le, H., Liu, L., Yue, X., et al., 2008. The midlatitude f2 layer during solar eclipses: Observations and modeling. J. Geophys. Res.: Space Phys. 113, A08309. https://doi.org/10.1029/2007JA013012.

Liu, J.Y., Hsiao, C.C., Tsai, L.C., et al., 1998. Vertical phase and group velocities of internal gravity waves derived from ionograms during the solar eclipse of 24 october 1995. J. Atmos. Solar Terr. Phys. 60 (17), 1679–1686. https://doi.org/10.1016/S1364-6826(98)00103-5.

Manju, G., Madhav Haridas, M.K., Ramkumar, G., et al., 2014. Gravity wave signatures in the dip equatorial ionosphere-thermosphere system during the annular solar eclipse of 15 january 2010. J. Geophys. Res.: Space Phys. 119 (6), 4929–4937. https://doi.org/10.1002/2014JA019865.

Manju, G., Sridharan, R., Ravindran, S., et al., 2012. Rocket borne in-situ electron density and neutral wind measurements in the equatorial ionosphere-results from the january 2010 annular solar eclipse campaign from india. J. Atmos. Solar Terr. Phys. 86, 56–64. https://doi.org/10.1016/j.jastp.2012.06.009.

Müller-Wodarg, I.C.F., Aylward, A.D., Lockwood, M., 1998. Effects of a mid-latitude solar eclipse on the thermosphere and ionosphere - a modelling study. Geophys. Res. Lett. 25 (20), 3787–3790. https://doi.org/10.1029/1998GL900045.

Nayak, C., Yigit, E., 2018. Gps-tec observation of gravity waves generated in the ionosphere during 21 august 2017 total solar eclipse. J. Geophys. Res.: Space Phys. 123 (1), 725–738. https://doi.org/10.1002/2017JA024845.

Nayak, C.K., Tiwari, D., Emperumal, K., et al., 2012. The equatorial ionospheric response over tirunelveli to the 15 january 2010 annular solar eclipse: Observations. Ann. Geophys. 30 (9), 1371–1377. https://doi.org/10.5194/angeo-30-1371-2012.

Panda, S.K., Gedam, S.S., Rajaram, G., et al., 2015. Impact of the 15 january 2010 annular solar eclipse on the equatorial and low latitude ionosphere over the indian region. J. Atmos. Solar Terr. Phys. 135, 181–191. https://doi.org/10.1016/j.jastp.2015.11.004.

Patra, A.K., Choudhary, R.K., 2009. Solar eclipse-induced e-region plasma irregularities observed by the gadanki radar. Geophys. Res. Lett. 36 (13), L13105. https://doi.org/10.1029/2009GL038669.

Patra, A.K., Pavan Chaitanya, P., Tiwari, D., 2011. Characteristics of 150 km echoes linked with solar eclipse and their implications to the echoing phenomenon. J. Geophys. Res.: Space Phys. 116, A05319. https://doi.org/10.1029/2010JA016258.

Rishbeth, H., 1968. Solar eclipses and ionospheric theory. Space Sci. Rev. 8 (4), 543–554. https://doi.org/10.1007/BF00175006.

Rocken, C., Kuo, Y.H., Schreiner, W.S., et al., 2000. Cosmic system description. Terrestrial, Atmospheric Oceanic Sci. 11 (1), 21–52. https://doi.org/10.3319/TAO.2000.11.1.21(COSMIC).

Šauli, P., Roux, S.G., Abry, P., et al., 2007. Acoustic-gravity waves during solar eclipses: Detection and characterization using wavelet transforms. J. Atmos. Solar Terr. Phys. 69 (17–18), 2465–2484. https://doi.org/10.1016/j.jastp.2007.06.012.

Sridharan, R., Devasia, C.V., Jyoti, N., et al., 2002. Effects of solar eclipse on the electrodynamical processes of the equatorial ionosphere: A case study during 11 august 1999 dusk time total solar eclipse over india. Ann. Geophys. 20 (12), 1977–1985. https://doi.org/10.5194/angeo-20-1977-2002.

St.-Maurice, J.-P., Ambili, K.M., Choudhary, R.K., 2011. Local electrodynamics of a solar eclipse at the magnetic equator in the early afternoon hours. Geophys. Res. Lett. 38 (4), L04102. https://doi.org/10.1029/2010GL046085.

Taori, A., Sathishkumar, S., Gurubaran, S., 2010. Variations in low-latitude middle atmospheric thermal structure during the 15 january 2010 solar eclipse. Current Sci. 99 (11), 1578–1581.

Torrence, C., Compo, G.P., 1998. A Practical Guide to Wavelet Analysis. Bull. Am. Meteorol. Soc. 79 (1), 61–78. https://doi.org/10.1175/1520-0477(1998)079<0061:APGTWA>2.0.CO;2.

Van Zandt, T.E., Norton, R.B., Stonehocker, G.H., 1960. Photochemical rates in the equatorial f 2 region from the 1958 eclipse. J. Geophys. Res. 65 (7), 2003–2009. https://doi.org/10.1029/JZ065i007p02003.

Vyas, B.M., Sunda, S., 2012. The solar eclipse and its associated ionospheric tec variations over indian stations on january 15, 2010. Adv. Space Res. 49 (3), 546–555. https://doi.org/10.1016/j.asr.2011.11.009.

Zhang, S.R., Erickson, P.J., Goncharenko, L.P., et al., 2017. Ionospheric bow waves and perturbations induced by the 21 august 2017 solar eclipse. Geophys. Res. Lett. 44 (24), 12067–12073. https://doi.org/10.1002/2017GL076054.